

RADIATION BEHIND THE STRONG SHOCK WAVES: EXPERIMENT AND MODELLING

E.M.Anohin, T.Yu.Ivanova, A.Yu.Starikovskii
Physics of Nonequilibrium Systems Laboratory
Moscow Institute of Physics and Technology, Dolgoprudny, 141700, Russia

Abstract

Spectral distribution in the visible and vacuum ultraviolet range in the Ar:CO₂:N₂ mixture was obtained over the wide shock wave velocity range. The role of the vacuum ultraviolet emission in the radiative heat transfer was investigated. On this basis the state-to-state kinetic scheme had been built. The results of numerical modelling was compared with experimental ones.

Introduction

In view of elaboration manned space activities a variety of investigation problems arises. At present time a Martian reentry space vehicle is being developed by American (NASA) and European (ESA) space agencies. In an effort to save on correlation effective weight/fuel the aerocapture is planned to use. So the heat shielding matter occurs striking actual. For decrease thermal shield mass the least calorific intensive trajectory must be estimated on the assumption of hypersonic velocities and rarefied atmosphere. Emission contribution to heat transfer can be significant under such conditions and amounts to tens percents. Under situation of high velocities and low densities the main area of emission is non-equilibrium area. Consequently chemical reactions carry against the background of incomplete vibrational relaxation processes. Martian atmosphere consists mainly of CO₂ and small-scale impurities, such as N₂, Ar, H₂ and so on. Experimental data can help us to evaluate emission contribution to heat transfer. At the same time with experimental data obtaining it is necessary to work out the kinetic scheme of reactions behind shock wave front. For the experimental data obtaining in mixtures similar to Martian atmosphere the emission behind shock wave front was observed. The results allow us to analyze emission spectra in vacuum ultraviolet and visible regions. As it was said, the distinctive feature of processes after shock wave front at high speed is chemical reactions passing with incomplete vibrational relaxation. So state-to-state kinetic must be used to sufficiently describe processes pattern after shock wave front. Also the translational and vibrational temperatures and kinetic curves of the mixture components were calculated at different temperatures and initial mixture components.

Experimental setup

For investigation of radiative heat transfer for hypersonic flow the shock tubes are the typical implement. We use steel one-diaphragm circular section shock tube with inner diameter 75mm. It consists of high pressure section(HPS), low pressure section(LPS) and expansion volume(fig.1). Before the experiment low pressure section is pumped out to 10⁻² torr and then is filled with investigated mixture. Different gas mixtures: one close to the Mars atmosphere, CO₂:N₂ mixture diluted in Ar and CO₂:N₂ mixture were used. The emission spectra after incident shock wave were studied. In order to avoid reflected shock wave expansion volume was used. It was divided by diaphragm against low pressure section. High pressure section can be used with pneumatic and explosive regimes to obtain wide velocity range (1.5-8 km/s). In case of explosive regime stoichiometric H₂:O₂ mixture diluted with He was used. The pressure in high pressure section at the beginning of the experiment was equal to 10 atmosphere. Due to a such regime high shock wave velocities were achieved. These velocities corresponded to the real reentry vehicles velocities during the entrance to upper layers of atmosphere. The shock wave front velocity measurements were carried out using two schlieren gauges, with 890 mm distance between them. The signals from these gauges were registered by the Tektronix TDS 2014 digital oscilloscope.

The diagnostic system consisted of modified spectrometer with a set of diffraction grids 37.5 G/mm, 750 G/mm, 1500 G/mm and streak camera C5680 Hamamtsu. The C5680 streak camera has high-sensitivity streak tube with a very high detection capability. This camera allows us to get the radiation spectral distribution over wide spectral range and temporal distribution at once. In our experiments we used camera observation time of 10-100 ns, it is sufficient to observe entire radiative region behind the

shock wave. The preliminary trigger signal is necessary for streak camera scanning initiation. As such signal the schlieren gauge's signal can be used. But the schlieren signal amplitude varieties for different gas mixture. Particularly its value is less for pure CO_2 and N_2 rather than for Ar. So stable streak camera triggering is problematic. Therefore in Ar experiments streak camera was triggered by schlieren gauge's signal, but in $\text{CO}_2:\text{N}_2$ experiments it was triggered by PeM-100 producing more intensive signal in shock wave front passing. The streak camera regime was chosen to obtain the most detailed data about spectral distribution and temporal dynamic of shock wave emission so that the radiating zone between shock wave front and contact surface was kept within measuring time of streak camera.

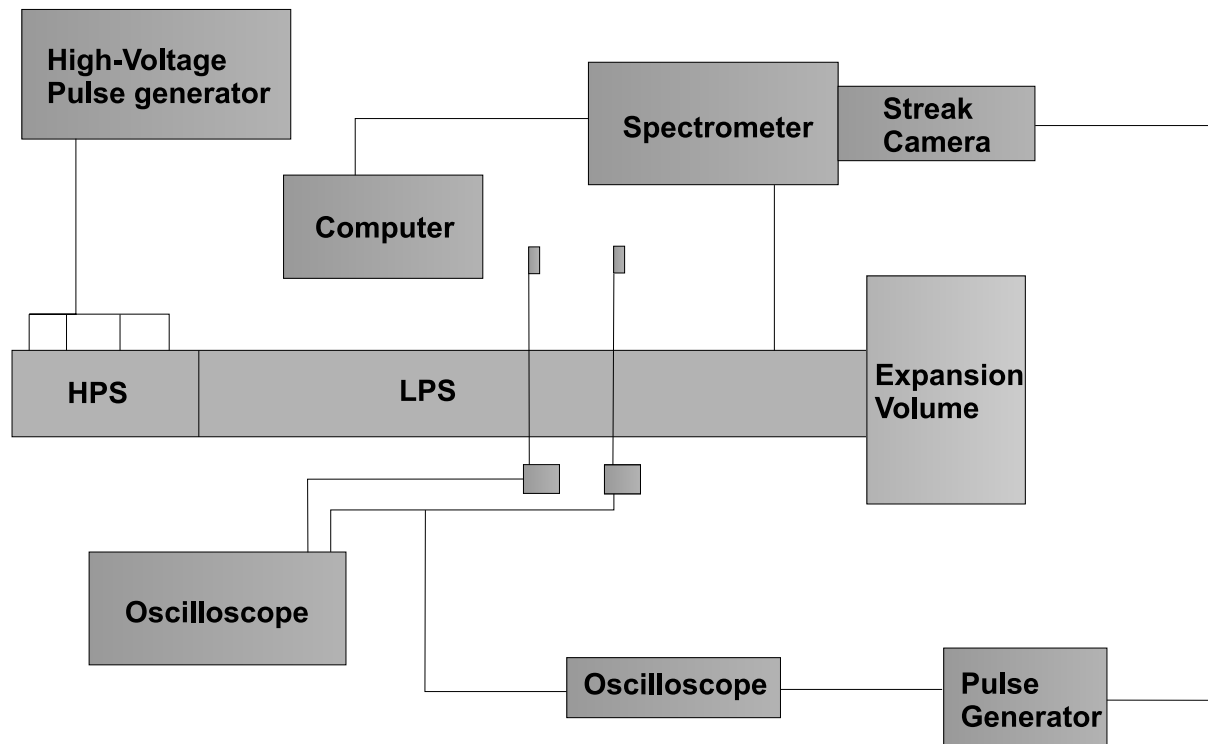


Figure 1: Block-scheme of experimental setup.

Streak camera measurements

The experiments were carried out in the and Ar: $\text{CO}_2:\text{N}_2$ (90:9.7:0.3) mixture, that is Martian atmosphere 10 times diluted with argon, and $\text{CO}_2:\text{N}_2$ (1:1) mixture. The shock wave velocities in the mixture were in the range of 3.5-6 km/s. As we used spectrometer with removable grids, the spectral range was 350 nm with 37.5 G/mm, 20 nm with 750 G/mm and 10nm with 1500 G/mm. We have measured spectral distribution over 300-660 nm and over CN-violet band. The pattern of emission after shock wave front was observed. The experiments helped us to investigate emission spectra of the mixture behind the reflected shock wave in a visible range of spectrum to separate the most bright and informative bands for the diagnostic of gas emission(fig2). So one can see from the emission spectral distribution that in this region CN-violet and C_2 -Swan play the major role.

For the refinement of spectral bands the measurements with 750 lines per millimeter and 1500 lines per millimeter were performed. For example in fig.3 the structure of CN-violet band is shown. It was necessary to make the series of experiments at different relation between investigated gases with 37.5 grid for checkout of kinetic model of processes after shock wave front in $\text{CO}_2:\text{N}_2$ and $\text{CO}_2:\text{N}_2:\text{Ar}$ mixtures. The experimental data could help us to confirm the values of chemical reaction constants and monitor the trend of kinetic curves.

Also in 750 G/mm and 1500 G/mm experiments it was shown that the most bright area is near the wave-front region (fig.4).

The most interesting area is the high velocity experiments, because they could render the pattern of vehicle entering in upper atmosphere layer. The same $\text{CO}_2:\text{N}_2$ and $\text{CO}_2:\text{N}_2:\text{Ar}$ mixtures were used. But

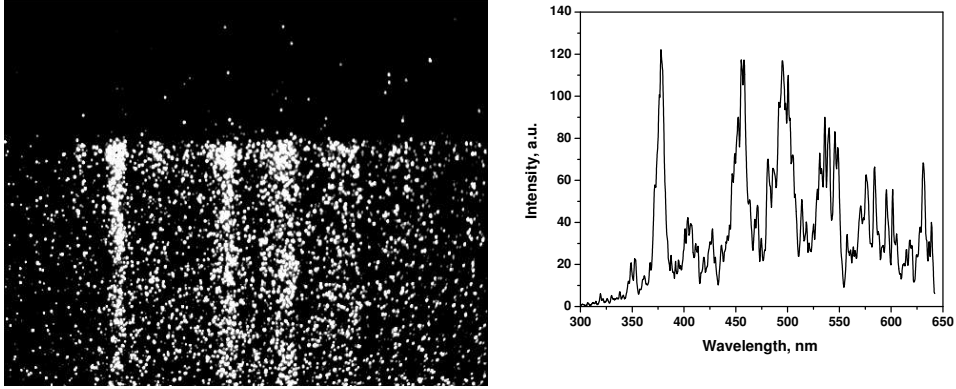


Figure 2: Ar:CO₂:N₂ experimental data and average spectrum, shock wave velocity $V=4.12$ km/s.

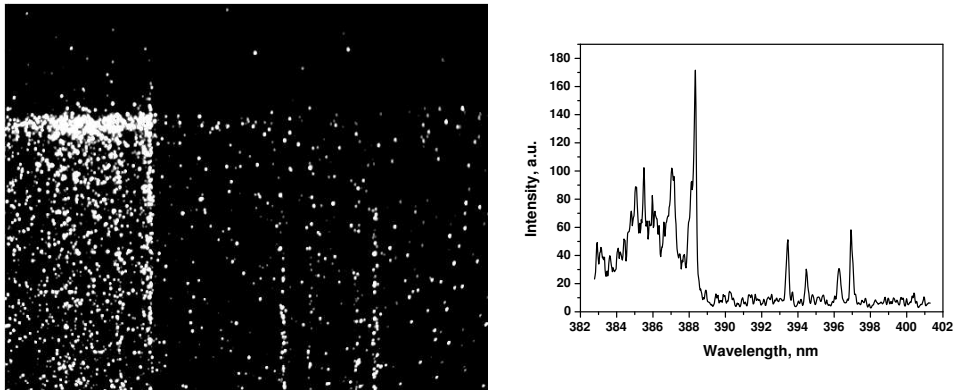


Figure 3: Ar:CO₂:N₂ experimental data and CN-violet band spectrum 0→0 transition, shock wave velocity $V=4.12$ km/s.

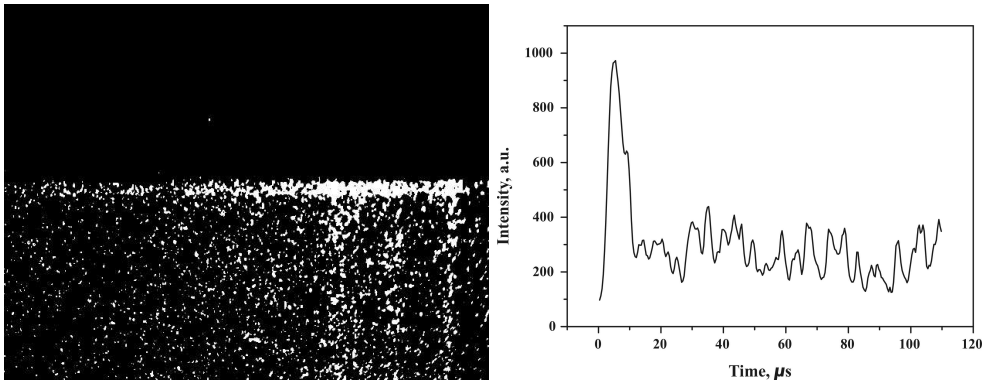


Figure 4: Ar:CO₂:N₂ experimental data and emission temporal dynamic, shock wave velocity $V=4.32$ km/s.

the significant discrepancy was revealed between different mixtures results under such conditions. As it is shown in fig. 5 and fig. 6 there were bright CN-violet spectral bands in CO₂:N₂ mixture and the nearly continuous spectrum in CO₂:N₂:Ar mixture at velocities 4.8-6.25 km/s. So we could assume that in high-velocity experiments we shouldn't use Ar diluted mixtures and change to mixtures close to Mars atmosphere composition.

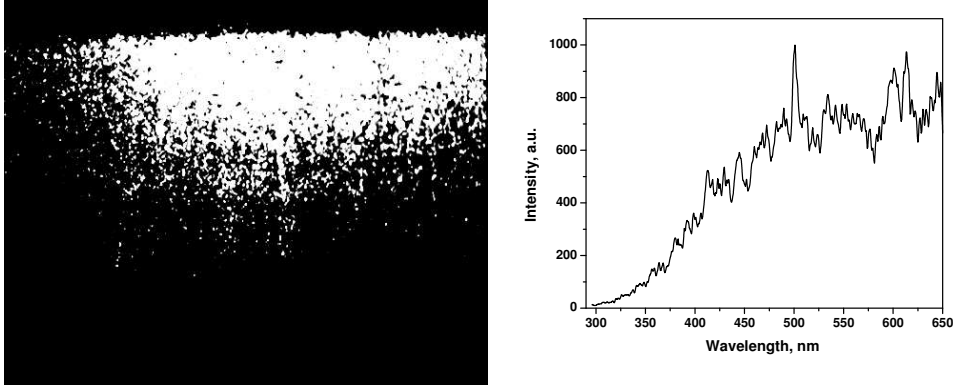


Figure 5: Ar:CO₂:N₂ experimental data and average spectrum, shock wave velocity $V=4.8$ km/s.

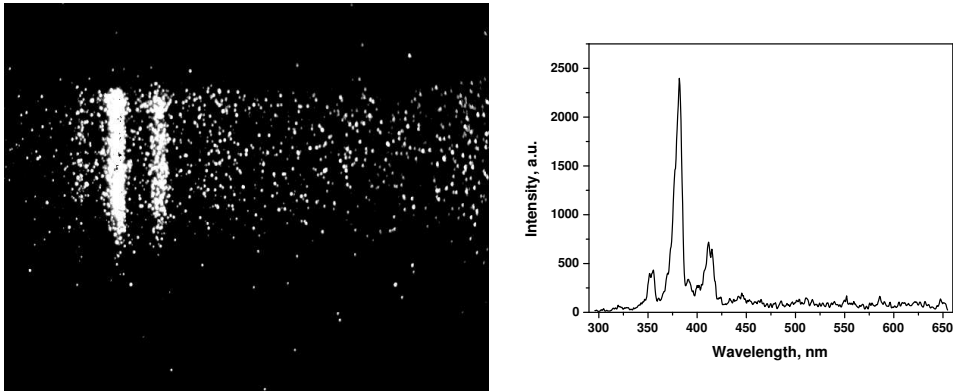


Figure 6: CO₂:N₂ experimental data and average spectrum, shock wave velocity $V=6.25$ km/s.

Vacuum ultraviolet emission of Ar:CO₂:N₂ mixture behind the strong shock wave

The experiments with gas radiation under the microwave discharge at different gas pressures demonstrated significant role of VUV region of spectrum in total radiation balance [1]. Experimental measurements in VUV spectral range were performed with the help of shock tube. The explosive regime of the shock tube was exploited to obtain wide velocity range (3.3-6.6 km/s), with shock wave front velocity measured by two schlieren gauges. We investigated CO₂:N₂ mixture diluted with Ar. The emission spectra after incident shock wave were studied. The emission diagnostic system consisted of vacuum monochromator McPherson 234/302 and photomultiplier with wide spectral sensitive photocathode which allowed us to get information in VUV spectral range. The PM signal was reproduced by digital oscillograph Tektronix TDS 2014, so temporal distribution of emission signal could be observed. Turbomolecular and forvacuum pumps supported required conditions for diagnostic. MgF₂ diagnostic window was installed into the shock tube diagnostic section to observe VUV spectral range. The intensity dependence on shock wave front velocity and on wavelength was investigated (fig. 7, 8). The significant increase of emission was observed in VUV area, as it was suspected. The maximum of emission accounted for wavelength about 170 nm. To obtain the quantitative calibration the following calibration method was used. First we obtained calibration in the visible spectral range, for that purpose we used monochromator and photomultiplier, lamp with tungsten filament was taken as a standard light source. Its temperature at current 22.75 A corresponds to 3000 K. Second, it was necessary to obtain absolute units of measurements at VUV area. For this aim before the VUV experiments visible range PM and VUV PM were adjusted for the same wavelength at ultraviolet spectral range and the values of the signals were compared to each other. Since we know the sensitivity curves for VUV photomultiplier and VUV monochromator we can derive the absolute units (Watts) in the VUV region. Then we took into account our shock tube emission geometry and divided given Watts into number of particles immediately behind the shock wave front.

In the fig. 8 there are two types of experiments with different shock wave intensity (different amount H₂:O₂ mixture in the high pressure section). For us it means that we have obtained the same velocities

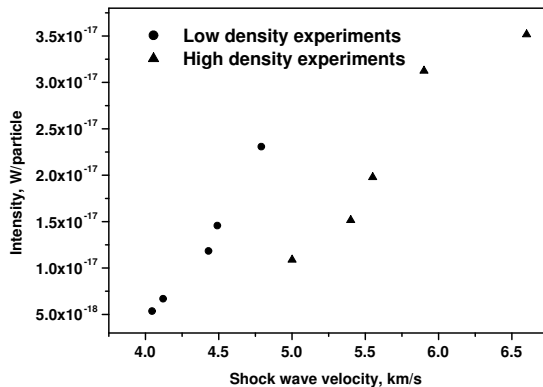


Figure 7: Intensity dependence on shock wave velocity in Ar:CO₂:N₂ mixture, wavelength 175 nm, $\Delta\lambda=9.6$ nm.

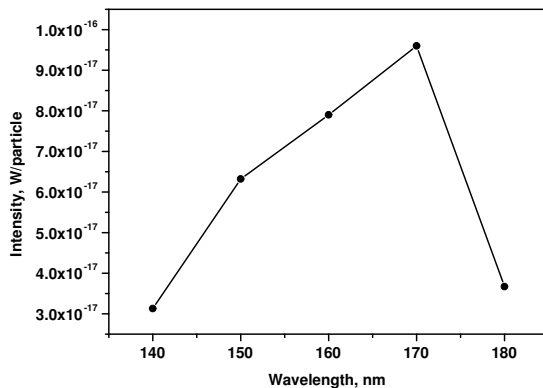


Figure 8: Intensity dependence on wavelength in Ar:CO₂:N₂ mixture, shock wave velocity $V=5.88$ km/s, $\Delta\lambda=9.6$ nm.

under different initial pressures i.e.different density behind the shock wave.

Kinetic scheme

To describe the chemical and physical processes behind the shock wave, the kinetic scheme, based on the state-to-state approach was developed. It means that we consider every vibrational level of the neutral molecule as a new species. The main species of this scheme are: N₂, O₂, C₂, CO, CN, CO₂, NO, O, C, N, C⁺, O₂⁺, CO⁺, O⁺, NO⁺. Also, to control the radiation emission, some electronically excited species such as CN(A²Π), CN(B²Σ⁺), C₂(d³Π_g), CO(A¹Σ⁺) and CO(b³Σ⁺) were included into the scheme. Initially we also considered some additional electronically excited species: CO⁺(A²Σ⁺) and CO⁺(B²Σ⁺), but numerical computations showed that their input to radiation heat transfer was negligible, so they were removed from our kinetic scheme. For accurate modelling vibrational relaxation processes, we consider neutral molecules as anharmonic oscillators, for this purpose we consider 48 energy levels for N₂, 32 levels for O₂, 36 levels for C₂, 66 levels for CO, 41 levels for CN, 38 levels for NO. CO₂ is a three-atomic molecule, so we consider 31, 69 and 37 energy levels for symmetric, deformation and anti-symmetric types of vibrations respectively. Chemical reaction rate constants and probabilities for vibrational 1→0 transitions were taken from extrapolated low temperature (up to 5 000 K) experimental data, n→n-1 transitions were calculated using SSH model of vibrational relaxation. The main chemical reactions of our kinetic scheme is shown in the Table 1.

In the fig. 9 one can see the results of our scheme calculations, there are mole fractions of neutral and charged particles behind the shock wave depending on the laboratory time. Also with the help

Table 1: Chemical reactions of the kinetic scheme.

<p>Dissociation</p> $\text{CO}_2 + \text{M} \leftrightarrow \text{CO} + \text{O} + \text{M}$ $\text{N}_2 + \text{M} \leftrightarrow 2\text{N} + \text{M}$ $\text{O}_2 + \text{M} \leftrightarrow 2\text{O} + \text{M}$ $\text{CO} + \text{M} \leftrightarrow \text{C} + \text{O} + \text{M}$ $\text{NO} + \text{M} \leftrightarrow \text{N} + \text{O} + \text{M}$ $\text{C}_2 + \text{M} \leftrightarrow 2\text{C} + \text{M}$ $\text{CN} + \text{M} \leftrightarrow \text{C} + \text{N} + \text{M}$	<p>Ionization</p> $\text{O} + \text{e} \leftrightarrow \text{O}^+ + \text{e} + \text{e}$ $\text{C} + \text{e} \leftrightarrow \text{C}^+ + \text{e} + \text{e}$ $\text{N} + \text{O} \leftrightarrow \text{NO}^+ + \text{e}$ $\text{O} + \text{O} \leftrightarrow \text{O}_2^+ + \text{e}$ $\text{C} + \text{O} \leftrightarrow \text{CO}^+ + \text{e}$
<p>Charge Transfer</p> $\text{O}_2 + \text{C}^+ \leftrightarrow \text{O}_2^+ + \text{C}$ $\text{CO} + \text{C}^+ \leftrightarrow \text{CO}^+ + \text{C}$ $\text{NO}^+ + \text{C} \leftrightarrow \text{NO} + \text{C}^+$ $\text{O}_2^+ + \text{O} \leftrightarrow \text{O}_2 + \text{O}^+$ $\text{NO}^+ + \text{N} \leftrightarrow \text{N}_2 + \text{O}^+$ $\text{NO}^+ + \text{O} \leftrightarrow \text{O}_2^+ + \text{N}$ $\text{CO} + \text{NO}^+ \leftrightarrow \text{CO}^+ + \text{NO}$ $\text{O}_2 + \text{NO}^+ \leftrightarrow \text{O}_2^+ + \text{NO}$ $\text{CO} + \text{O}_2^+ \leftrightarrow \text{CO}^+ + \text{O}_2$	<p>Bimolecular Reactions</p> $\text{NO} + \text{O} \leftrightarrow \text{N} + \text{O}_2$ $\text{N}_2 + \text{O} \leftrightarrow \text{NO} + \text{N}$ $\text{CO} + \text{O} \leftrightarrow \text{C} + \text{O}_2$ $\text{CO} + \text{C} \leftrightarrow \text{C}_2 + \text{O}$ $\text{CO} + \text{N} \leftrightarrow \text{CN} + \text{O}$ $\text{N}_2 + \text{C} \leftrightarrow \text{CN} + \text{N}$ $\text{CN} + \text{O} \leftrightarrow \text{NO} + \text{C}$ $\text{CN} + \text{C} \leftrightarrow \text{C}_2 + \text{N}$ $\text{CO}_2 + \text{O} \leftrightarrow \text{O}_2 + \text{CO}$ $\text{CO} + \text{N} \leftrightarrow \text{NO} + \text{C}$ $\text{CO} + \text{CO} \leftrightarrow \text{CO}_2 + \text{C}$ $\text{NO} + \text{CO} \leftrightarrow \text{CO}_2 + \text{N}$
<p>Electron excitation and quenching</p> $\text{CN}(X^2\Sigma^+) + \text{M} \leftrightarrow \text{CN}(B^2\Sigma^+) + \text{M}$ $\text{CN}(X^2\Sigma^+) + \text{M} \leftrightarrow \text{CN}(A^2\Pi) + \text{M}$ $\text{CO}(X^1\Sigma^+) + \text{M} \leftrightarrow \text{CO}(A^1\Pi) + \text{M}$ $\text{CO}(X^1\Sigma^+) + \text{M} \leftrightarrow \text{CO}(B^1\Sigma^+) + \text{M}$ $\text{C}_2(X^1\Sigma^+) + \text{M} \leftrightarrow \text{C}_2(d^3\Pi_g) + \text{M}$	
<p>Radiation processes</p> $\text{CN}(B^2\Sigma^+) \rightarrow \text{CN}(X^2\Sigma^+) + h\nu$ $\text{CN}(A^2\Pi) \rightarrow \text{CN}(X^2\Sigma^+) + h\nu$ $\text{C}_2(d^3\Pi_g) \rightarrow \text{C}_2(a^3\Pi_u) + h\nu$ $\text{CO}(A^1\Pi) \rightarrow \text{CO}(X^1\Sigma^+) + h\nu$ $\text{CO}(B^1\Sigma^+) \rightarrow \text{CO}(X^1\Sigma^+) + h\nu$ $\text{CO}(B^1\Sigma^+) \rightarrow \text{CO}(A^1\Pi) + h\nu$	

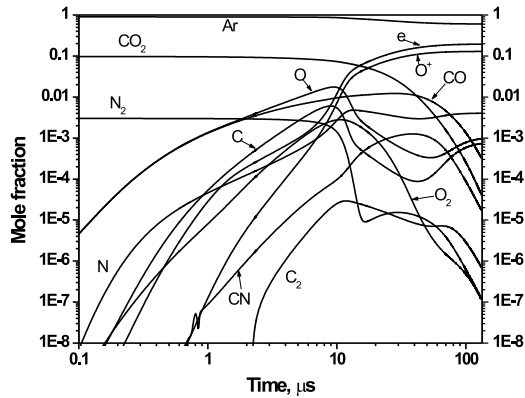


Figure 9: Mole fraction of the main species in the Ar:CO₂:N₂ mixture, corresponds to shock wave velocity $V=7.68$ km/s and initial pressure 0.1 torr.

of our kinetic scheme we can describe the processes inside the nonequilibrium relaxation region more

correctly than using two-temperature approach. The difference between these two models at different times is shown in the fig. 11. The difference from equilibrium at those times is shown in the fig. 10. The calculations correspond to 0.1 atm pressure and 15 000 K translational temperature behind the shock wave front in the $\text{CO}_2:\text{N}_2$ (1:1) mixture. We can see that population of the highest vibrational levels inside the relaxation region differ from each other in two orders of magnitude in the different models. As far as dissociation mostly comes from highest vibrational levels, we have to use state-to-state kinetic model to describe at least nonequilibrium relaxation region.

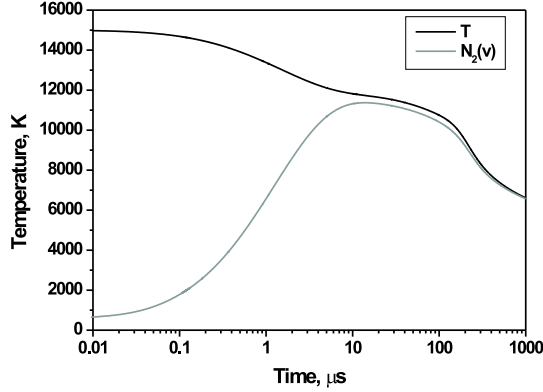


Figure 10: Translational and vibrational temperature behavior, vibrational temperature is calculated using first and zero vibrational level population.

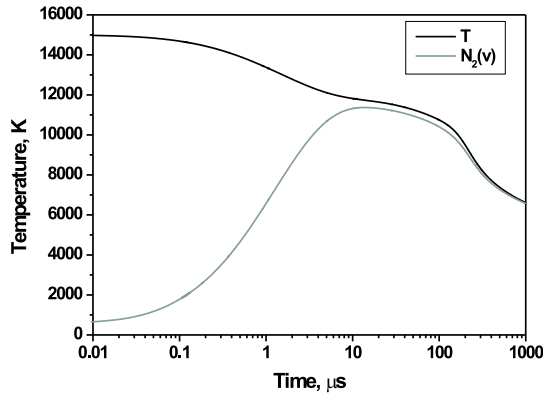


Figure 11: Nitrogen energy level population for the different moments of time, low curve - 0.1 μs , middle curve - 1 μs , upper curve - 10 μs (black curves - population calculated using state-to-state kinetics, gray dash-dotted curves - two-temperature approximation)

In the fig. 12 the comparison between experimental and calculated emission is provided. The experimental curves 3 and 4 are obtained from photomultipliers which were adjusted to 175 and 388 nm with $\Delta\lambda=9.6$ nm. Experimental and calculated emission values of CN-violet band are in a good agreement, the excess of experimental radiation in the peak tail can be explained by continuous spectrum emission which was not taken into account in our calculations. The discrepancy between experimental and calculated CO emission is more significant. This discrepancy is due to lack of information about CO high temperature kinetic.

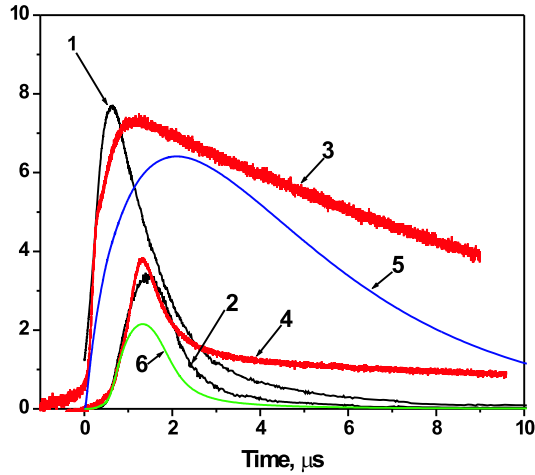


Figure 12: Comparison between experimental and calculated emission dynamics, $V_s=5.9$ km/s $P_1=2$ torr; 1,2 - calculated emission of CO(4+) and CN(violet) respectively; 3,4 - Experimental emission on $\lambda=175$ nm and $\lambda=388$ nm ($\Delta\lambda=9.6$ nm); 5,6 - calculated molar fraction of CO and CN respectively

Conclusions

The spectral distribution in the Ar:CO₂:N₂ mixture over the wide range of shock wave velocity was investigated, these data were used to create state-to-state kinetic scheme. Also it was noticed that the most radiative region is near front emission. For high shock wave velocities it was obtained that in the Ar:CO₂:N₂ mixture the continuous spectrum plays major role, that is not the case in the CO₂:N₂ mixture, it seems that for high shock wave velocities one have to use undiluted Martian atmosphere. The intensity of the vacuum ultraviolet region was measured and compared with intensity in the visible spectral range. The state-to-state kinetic scheme had been built, the mole fractions of the mixture species were calculated under the different conditions. It was shown that in the nonequilibrium relaxation region we can not use two-temperature approximation, because of the nonequilibrium vibrational levels population. Also comparison between experimental and numerical radiation was made, it was shown that there is a good agreement in the visible spectral region (in the case of CN-violet band). For correct consideration of emission in the VUV region additional experimental investigation about CO high temperature kinetic should be provided.

Acknowledgments

This work was partially supported under Project No 1440 of International Science and technology Center and Russian Ministry for Science and High Education.

References

- [1] E.M. Anokhin, S.M.Starikovskaia, A.Yu.Starikovskii. Energy transfer in hypersonic plasma flow and flow structure control by low temperature nonequilibrium plasma. 42nd AIAA Aerospace Sciences Meeting and Exhibit, Reno, Nevada, USA, 2004.